Melting heat transfer in magnetohydrodynamic radiative Williamson fluid flow with non-uniform heat source/sink

To cite this article: G Kumaran *et al* 2017 *IOP Conf. Ser.: Mater. Sci. Eng.* **263** 062022

IOP Conf. Series: Materials Science and Engineering **263** (2017) 062022 doi:10.1088/1757-899X/263/6/062022

Melting heat transfer in magnetohydrodynamic radiative Williamson fluid flow with non-uniform heat source/sink

G Kumaran[1], N Sandeep[1], R Vijayaragavan[2]

[1]Department of Mathematics, School of Advanced Sciences, VIT University, Vellore-632014, India
[2]Department of Mathematics, Thiruvalluvar University, Vellore-632115, India

E-mail: dr.nsrh@gmail.com

Abstract. We analyzed the influence of melting heat transfer in magnetohydrodynamic radiative Williamson fluid flow past an upper paraboloid of revolution with viscous dissipation. The overseeing flow and thermal distributions of insecure flow is introduced and streamlined utilizing comparable and nonsimilar transforms. The diminished coupled nonlinear differential equations are solved systematically with the assistance of a strong explanatory strategy, in particular, the shooting technique. Numerical solutions for the imperative physical channel are figured and shown. The physical components of reasonable parameters are examined through the graphs of skin friction, local Nusselt number. Rising values of Eckert number depreciate the flow and heat transfer rate.

Nomenclature.

A, b	non negative constants
m	velocity power index
C_{fx}	skin friction coefficient
q_w	heat transfer
U_w	stretching velocity at the wall
b_1	fluid thermal property
Ec	Eckert number
f, F	dimensionless velocity
Pr	Prandtl number
Nu_x	Nusselt number
S_t	thermal stratification.
A^*, B^*	non-uniform heat source/sink parameter

T	temperature of the fluid
R	thermal radiation
k_b	fluid thermal conductivity
C_s	concentration susceptibility
C_p	specific heat constant pressure

Dimensional parameter

B_0	magnetic field strength $\left(Kg/(S^2A)\right)$
k	fluidthermal conductivity $\left(w/mk\right)$
T_w	Surface fluid temperature
T_∞	free stream temperature
x, y	cartesian coordinates $\left(m\right)$
u, v	velocity components in x and y axis $\left(m/s\right)$

Greek Symbols

σ	fluid electrical conductivity
λ	stretching rate parameter
σ^*	Stefen-Boltzmann constant
k^*	mean absorption coefficient.
ζ	similarity variable
δ	melting parameter.
μ_b	plastic dynamic viscosity
ε	thermal conductivity parameter
θ, Θ	non dimensional temperature
τ	effective heat capacitance
ξ	stream function
ν	kinematic viscosity $\left(m^2/s\right)$
α	thermal diffusivity $\left(m^2/s\right)$
ρ	fluid density $\left(Kg/m^3\right)$
ρc_p	fluid thermal capacity $\left(J/\left(m^3k\right)\right)$

1. Introduction

The Magnetohydrodynamic flow of non-Newtonian fluid has achieved an incredible accomplishment in the hypothesis of fluid mechanics because of its applications in natural sciences and industry. A couple of utilizations of non-Newtonian fluids are nourishment blending and chyme development in the digestive tract, polymer arrangements, paint, stream of blood, the stream of atomic fuel slurries, the stream of fluid metals and combinations, a stream of mercury amalgams and oils with substantial oils and greases. Khan et al. [1] investigated the 2D laminar magnetohydrodynamic flow of Williamson fluid manifested with artificially receptive. The impact of radiation on magnetohydrodynamic Williamson fluid flow over a stretching sheet in the presence of preamble medium and chemical

reaction using R-K-F with shooting technique has been analyzed by Krishnamurty et al. [2]. Non-linear radiation influence on magnetohydrodynamic nanofluid flow past a stretching surface was discussed by Prasannakumara et al. [3] and found that the flow depreciates with enhancing the permeability parameter.

Bhatti and Rashidi [4] introduced the impact of Soret number on non-Newtonian nanofluid past a stretching surface in a preamble medium with thermal radiation. Nadeem and Hussain [5] studied the 2D magnetohydrodynamic Williamson nanofluid flow towards a stretching surface. Hyat et al. [6] studied the impact of unsteady hydromagnetic Williamson fluid towards a porous stretching surface in the presence of thermal radiation. And found that the increase in suction effect depreciates the momentum boundary layer thickness. Thermal radiation effects on magnetohydrodynamic nanofluid flow towards an incompressible stretching surface with buoyancy force have been discussed by Rashidi et al. [7]. Zeeshan et al. [8] investigated the heat transfer influence on the MHD flow of nanofluid towards a stretching surface with the magnetic dipole and observed that the rising values of Prandtl number enhances the friction factor. The influence of thermophoresis on magnetohydrodynamic nanofluid flow towards a two rotating flat plates alongwith thermal radiation using R-K Method was analyzed by Shikholeslami et al. [9]. Pal et al. [10] discussed the effects of Ohmic dissipation on magnetohydrodynamic non-Newtonian nanofluid flow past a non-linear stretching surface with thermal radiation. 2D magnetohydrodynamic flow over a vertical stretching surface in a preamble medium with thermal radiation was studied by Rashidi et al. [11].

Hayat et al. [12] investigated the influence of chemical reactions in MHD Jefffrey fluid flow past a stretched sheet with magnetic field. The influence of viscous dissipation in the MHD convective flow towards a non-isothermal wedge with heat source discussed by Chamkha et al. [13]. Cookey et al. [14] investigate the impact of thermal radiation on unpredictable magnetohydrodynamic flow over an interminable warmed vertical flat plate in a permeable medium. The magnetohydrodynamic stream and heat shift in a non-Newtonian fluid towards a stretching sheet was investigated by Siddheswar and Mahabaleswar [15].

The influence of Dufour effect on 2D magnetohydrodynamic flow over a stretching surface in the presence thermal radiation and magnetic field are studied by Raju [16] and found that diffusion-thermo helps to increase the temperature distribution. Mabood et al. [17] studied the impacts of thermo diffusion on convective magnetohydrodynamic micropolar fluid flow past an incomparable stretching surface. Krisha et al. [18] studied the chemical reaction influence on magnetohydrodynamic boundary layer flow past a vertical preamble plate in with heat source/sink. The unsteady 2D laminar convective flow of nanoparticle bounded by a vertical plate with preamble medium in a moving system was analytically discussed by Reddy et al. [19]. Raju et al. [20] analyzed the impacts of cross diffusion on heat transfer magnetichydrodynamic convective Couette flow towards a vertical plate with radiation using finite element method. By taking all the above reviews into thought in this study, we detailed on the magnetic field, thermal radiation, viscous dissipation and non-uniform heat source/sink impacts on MHD flow towards an upper part of parabolic of revolution. The overseeing PDE's of the flow are changed to ODE's by utilizing similarity transformation and after that tackled numerically.

2. **Mathematical formulation**

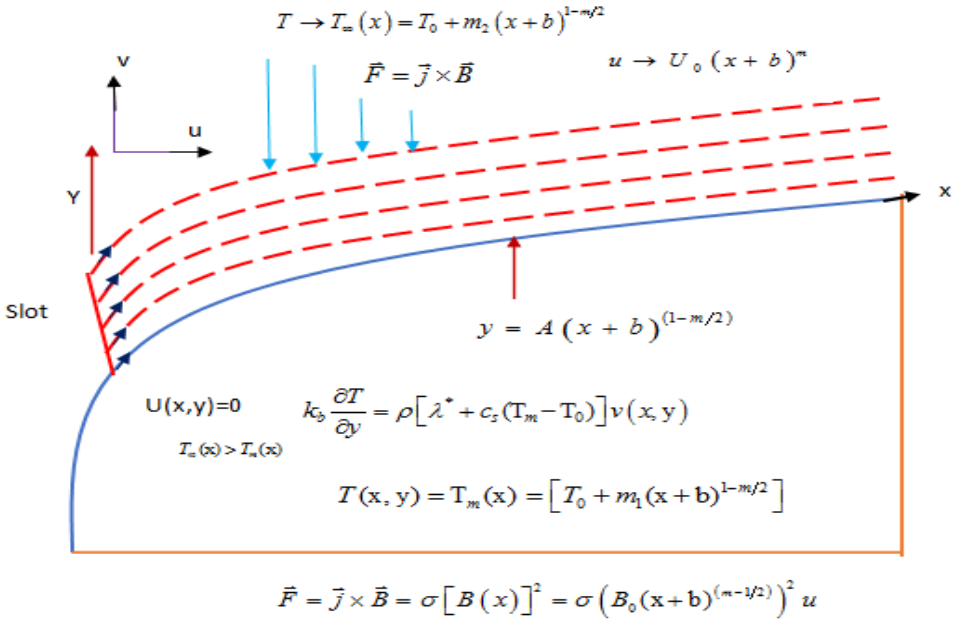

Figure1. Physical configuration

Consider the 2D laminar convective magnetohydrodynamic of Williamson fluid flow towards a paraboloid revolution in the presence of thermal radiation, exponential heat source and non-uniform heat source/sink. The stream is restricted over the area $A(x+b)^{\frac{m-1}{2}} \le y < \infty$ (here A and b are positive constants and $m<1$) and the revolving paraboloid are stretched with the velocity $U_w = U_0 (x+b)^m$. And flat surface is placed along x-direction and y-direction is normal to it. The magnetic field of strength $B(x) = B_0 (x+b)^{\frac{m-1}{2}}$ is applied in the flow axis as displayed in Fig.1. With the above assumptions and followed by the researchers Anjali Devi, Prakesh [21] and Animasaun [22]. The governing two dimensional flow equations are:

$$\frac{\partial^2 \xi}{\partial x \partial y} - \frac{\partial^2 \xi}{\partial y \partial x} = 0, \tag{1}$$

$$\frac{\partial \xi}{\partial y}\frac{\partial^2 \xi}{\partial x \partial y} - \frac{\partial \xi}{\partial x}\frac{\partial^2 \xi}{\partial y^2} = \frac{1}{\rho}\frac{\partial}{\partial y}\left(\mu_b(T)\frac{\partial^2 \xi}{\partial y^2}\right) + \sqrt{2v\Gamma}\frac{\partial^2 \xi}{\partial y^2}\left(\frac{\partial^3 \xi}{\partial y^3}\right) + g\gamma\frac{m+1}{2}(T_\infty - T) - \frac{\sigma B_0^2}{\rho}\frac{\partial \xi}{\partial y}, \tag{2}$$

$$\frac{\partial \xi}{\partial y}\frac{\partial T}{\partial x} - \frac{\partial \xi}{\partial x}\frac{\partial T}{\partial y} = \frac{1}{\rho c_p}\frac{\partial}{\partial y}\left(k_b(T)\frac{\partial T}{\partial y}\right) + \frac{\sigma B_0^2}{\rho c_p}\left(\frac{\partial \xi}{\partial y}\right)^2 + \frac{q'''}{\rho c_p} + \frac{\mu_b(T)}{\rho C_p}\frac{\partial^2 \xi}{\partial y^2}\frac{\partial^2 \xi}{\partial y^2}, \tag{3}$$

with the conditions

$$\left.\begin{aligned} &u = U_0 (x+b)^m,\ k_b(T)\frac{\partial T}{\partial y} = \rho\left[\lambda^* + c_s\left(T_m - T_0^*\right)\right] v(x,y), T = T_m(x) \quad at\ y = A(x+b)^{\frac{1-m}{2}}, \\ &T \to T_\infty(x) u \to 0, \quad as\ \ y \to \infty. \end{aligned}\right\} \tag{4}$$

The non-uniform heat source/sink, q''', is modeled as

$$q''' = \frac{k_f u(x)}{xv}\left(\left(T_\infty - T_0\right)A^* F' + \left(T - T_m\right)B^*\right) \tag{5}$$

Consider the modified mathematical models of $\mu_b(\mathrm{T})$ and K_b^* models proposed in [23] adopted in [24]

$$\mu_b(T) = \mu_b^*\left[1 + b_1\left(T_\infty - T\right)\right], k_b(T) = k_b^*\left[1 + b_2\left(T - T_m\right)\right] \tag{6}$$

$$T_m(x) = T_0 + m_1\left(x+b\right)^{\frac{1-m}{2}}, T_\infty(x) = T_0 + m_2\left(x+b\right)^{\frac{1-m}{2}} \tag{7}$$

$$T_\infty - T = \left(1-\Theta\right)\left[T_\infty - T_0\right] - m_1\left(x+b\right)^{\frac{1-m}{2}} \tag{8}$$

$$\left(T_m - T_0\right) = m_1\left(x+b\right)^{\frac{1-m}{2}}, \left(T_\infty - T_0\right) = m_2\left(x+b\right)^{\frac{1-m}{2}} \tag{9}$$

$$\delta = b_1\left(T_\infty - T_0\right), b_1\left(T_m - T_0\right) = \delta S_t, S_t = \frac{m_1}{m_2} \tag{10}$$

Similarity variables,

$$\left.\begin{aligned} &\zeta = y\left(\frac{m+1}{2}\frac{U_0}{\vartheta}\right)^{0.5}\left(x+b\right)^{\frac{m-1}{2}},\ \xi(x,y) = F(\zeta)\left(\frac{2}{m+1}\right)^{0.5}(vU_0)^{0.5}\left(x+b\right)^{\frac{m-1}{2}}, u = \frac{\partial \xi}{\partial y}, v = -\frac{\partial \xi}{\partial x},\\ &\Theta(\zeta) = \frac{T - T_m}{T_\infty - T_0}, \end{aligned}\right\} \tag{11}$$

The Rosseland approximation for radiation is given below

$$q_r = -\frac{4\sigma^*}{3k^*}\frac{\partial T^4}{\partial y} \tag{12}$$

We presume that temperature contrasts inside the flow are such that T^4 the term might be communicated as a linear function of thermal. This is proficient b extending T^4 in Taylor series regarding T_∞ and ignoring superior order expressions, thus

$$T^4 \cong 4T_\infty^3 T - 3T_\infty^4 \tag{13}$$

Eqn (3) reduces to

$$\frac{\partial \xi}{\partial y}\frac{\partial T}{\partial x} - \frac{\partial \xi}{\partial x}\frac{\partial T}{\partial y} = \frac{1}{\rho c_p}\frac{\partial}{\partial y}\left(k_b(T)\frac{\partial T}{\partial y}\right) + \frac{1}{\rho c_p}\frac{16\sigma^* T_\infty^3}{3k^*}\frac{\partial^2 T}{\partial y^2} + \frac{q'''}{\rho c_p} + \frac{\mu_b(T)}{\rho C_p}\frac{\partial^2 \xi}{\partial y^2}\frac{\partial^2 \xi}{\partial y^2}, \tag{14}$$

Substituting (5)-(11) into (1), (2), (4) and (14) becomes

$$\left.\begin{aligned} &\left[1 + \delta - \Theta\delta - \delta S_t\right]F''' + \lambda F''' F'' - \delta\Theta' F'' + FF'' - \frac{2m}{m+1}F'F'\\ &\qquad + F'\frac{2M}{m+1} + G_t\left[\left(1-\Theta\right)\delta - \delta S_t\right] = 0, \end{aligned}\right\} \tag{15}$$

$$\left.\begin{aligned} &\left[1 + \varepsilon\Theta - \frac{4}{3}R\right]\Theta'' + \varepsilon\Theta'\Theta' - \Pr S_t\frac{1-m}{1+m}F' + \Pr F\Theta' - \Pr\frac{1-m}{1+m}\Theta F' + \frac{2}{m+1}\Pr\left(A^* F' + B^*\Theta\right)\\ &\quad + \Pr E_c\frac{m+1}{2}\left[1 + \delta - \delta\Theta - \delta S_t\right]F'' F'' + \Pr E_c\frac{m+1}{2}\left[1 + \delta - \delta\Theta - \delta S_t\right]F'' F'' = 0, \end{aligned}\right\} \tag{16}$$

The dimensionless parameters are given by

$$\left.\begin{aligned} Ec=\frac{U_0(x+b)^{\frac{m+1}{2}}}{C_p(T_w-T_\infty)},\gamma=\frac{C_p m_2(x+b)^{\frac{1-m}{2}}}{\lambda^*+C_s m_1(x+b)^{\frac{1-m}{2}}},\mathrm{M}=\frac{\sigma B_0^2}{\rho U_0},\varepsilon=b_2(T_\infty-T_0),\\ \lambda=\sqrt{2}\Gamma B(x+b)^{\frac{3m-1}{2}},G_r=\frac{g\gamma}{b_1U_0^2(x+b)^{3m-1}},R=\frac{4\sigma^*}{k^*\nu}T_\infty^3 \end{aligned}\right\} \quad (17)$$

dimensionless boundary restrictions, y is not a least initial point of the slot, from this condition not satisfied Eq. (4) at $y=0$. y is not a suitable point to ζ . So we assumed $y=A(x+b)^{\frac{1-m}{2}}$ is least point of ζ as

$$\chi=A\left(\frac{(m+1)U_0}{2\vartheta}\right)^{0.5} \quad (18)$$

Which infers that at the wall, the restriction reasonable to scale the boundary layer flow is $\zeta=\eta$. The changed conditions are as follows:

$$\left.\begin{aligned} &\frac{dF}{d\zeta}=0,F(\chi)+\frac{\gamma[1+\Theta\varepsilon]}{\mathrm{Pr}}+\chi\frac{m-1}{m+1}\frac{dF}{d\chi}=0,\ \Theta(\chi)=0\ \ at\ \chi=\zeta\\ &\frac{dF}{d\zeta}\to 1,\Theta\to 1-S_t\ as\ \chi\to\infty. \end{aligned}\right\} \quad (19)$$

$$\mathrm{Pr}=\frac{\mu_b C_p}{k_b^*}=[1+\delta-\delta\Theta-\delta S_t]\frac{\mu_b^* C_p}{k_b^*}=\mathrm{Pr}[1+\delta-\delta\Theta-\delta S_t] \quad (20)$$

The domain transforms from $[\chi,\infty)$ to $[0,\infty)$ we assumed $f(\eta)=f(\zeta-\chi)$ and $\theta(\eta)=\theta(\zeta-\chi)$.

$$\left.\begin{aligned} &[1+\delta-\delta\theta-\delta S_t]f'''-\delta\theta' f''+\lambda f''' f''+ff''-\frac{2m}{m+1}f'f'\\ &\qquad+f'\frac{2M}{m+1}+G_r[(1-\theta)\delta-\delta S_t]=0, \end{aligned}\right\} \quad (21)$$

$$\left.\begin{aligned} &[1+\varepsilon\theta-]\theta''+\varepsilon\theta'\theta'+[1+\delta-\delta\theta-\delta S_t]\mathrm{Pr}\left(\begin{aligned}&-S_t\frac{1-m}{m+1}f'+f\theta'-\frac{1-m}{m+1}\theta f'\\&+\frac{2}{m+1}(A^*f'+B^*\theta)\end{aligned}\right)\\ &\qquad+\mathrm{Pr}\,Ec\frac{m+1}{2}[1+\delta-\delta\theta-\delta S_t]^2 f''f''=0, \end{aligned}\right\} \quad (22)$$

With boundary conditions

$$\left.\begin{aligned} &\frac{df}{d\eta}=0,f(\eta)+\frac{\gamma}{\mathrm{Pr}[1+\delta-\delta S_t]}\theta'+\chi\frac{m-1}{m+1}\frac{df}{d\eta}=0,\ \theta(\eta)=0\ \ at\ \eta=0,\\ &\frac{df}{d\eta}\to 1,\theta(\eta)\to 1-S_t\ as\ \eta\to\infty. \end{aligned}\right\} \quad (23)$$

The amounts of intrigue are the flow coefficient C_{fx} and reduced Nusselt number Nu_x.

$$C_{f_x}=\frac{\tau_w}{\rho\sqrt{\frac{m+1}{2}}U_0^2},N_{u_x}=\frac{(x+b)q_w}{k_b(T_\infty-T_0)\sqrt{\frac{m+1}{2}}} \quad (24)$$

Where τ_w is the shear stress between Williamson fluid and q_w is the heat flux at all points on the surface

$$\tau_w = -\left.\frac{\partial u}{\partial y}\right|_{y=A(x+b)^{1-m/2}}, q_w = -\left.\left(k_b \frac{\partial T}{\partial y}\right)\right|_{y=A(x+b)^{1-m/2}} \quad (25)$$

$$\mathrm{Re}_x^{1/2} C_{f_x} = f''(0), \; Nu_x \,\mathrm{Re}_x^{-1/2} = -\theta'(0), \quad (26)$$

where $R_{e(x)}$ is the reduced Reynolds number.

3. Results and Discussion

The reduced nonlinear ODE's Eqs. (21) and (22) with the boundary restrictions Eq. (23) are resolved by utilizing R-K based shooting technique for the different parameters viz. magnetic field, thermal stratification, melting parameter, temperature dependent thermal conductivity, Ec, A^*, B^*, R and velocity power index on the velocity and temperature profile. In this study, we considered the pertinent parameter values as $S_t = 0.3, \delta = .05,\ \varepsilon = 0.1, \mathrm{S} = 0.2, \mathrm{K} = 0.3, m = 0.8, \mathrm{Pr} = 4, \mathrm{A}^* = 0.1 = \mathrm{B}^*,\ \mathrm{Gr} = 1,$ $\mathrm{M} = 0.5, \lambda = 0.5 = R.$ These values are unchanging for the entire study unless otherwise particularized in the corresponding tables and plots. Figures 2 and 3 displayed the impact of M on flow and temperature distributions respectively. We noticed that the boosting values of M enhances the velocity profiles and mixing behavior on thermal distribution. Generally, improving in M produce a reverse force to the flow is called as Lorenz force. The Lorenz force may be control to the flow and lessen the velocity distribution as well as it helps to enhance the temperature distribution. Figure 4 display that the impact of Ec on thermal distribution. We found that the rising values of Eckert number increasing the thermal profile. Figure 5 shows the effects of R on temperature profile. We noticed that the improving value of radiation parameter depreciates the thermal distribution profile.

Figures 6 and 7 display the impact of A^* and B^* on thermal profiles. We observed that the rising value of A^* and B^* with increase the thermal profiles. Physically, the non-negative values of heat source/sink acts as heat creaters, which discharge the heat to the flow. For this reason we observe improvement in the thermal distribution. Figures 8 and 9 shows that the impact of λ on flow and thermal distributions. We noticed that the rising values of λ enhanced the both momentum and thermal profiles. Figure. 10 depicts the impact of δ on thermal profile. We noticed that boosting value of δ enhances the thermal profile of Williamson fluid. Figure 11 illustrates the influence of S_t on temperature distribution. It is clear that the thermal distribution is decreasing for increasing values of S_t. Generally, S_t decreases the productive convective potential among the ambient fluid and the sheet. From these reason the thickness of the thermal layer lessens.

Table 1 demonstrates the variation in the flow and Nusselt number for Williamson fluid. We found that the increasing values of magnetic field parameter depreciate the flow and enhances the Nusselt number. Improving values of Ec, A^* and B^* increase both the skin friction and heat transfer. Rising values of λ and δ with increases the flow and depreciates the Nusselt number. Flow and heat transfer rate increasing for rising values of thermal radiation. Boosting values of S_t with lessen the flow and opposite in Nusselt number in Williamson fluid.

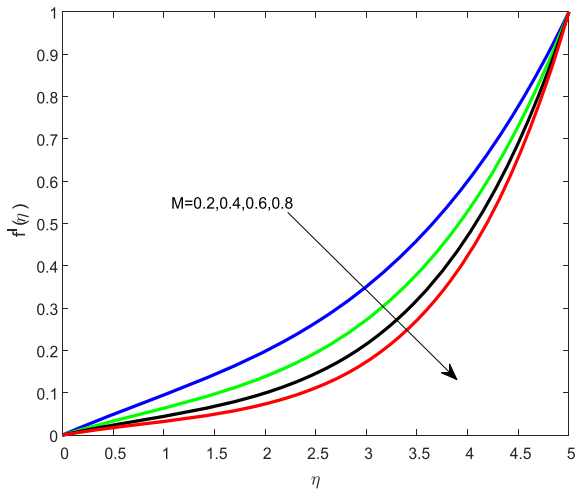

Figure 2. impact of M on $f'(\eta)$

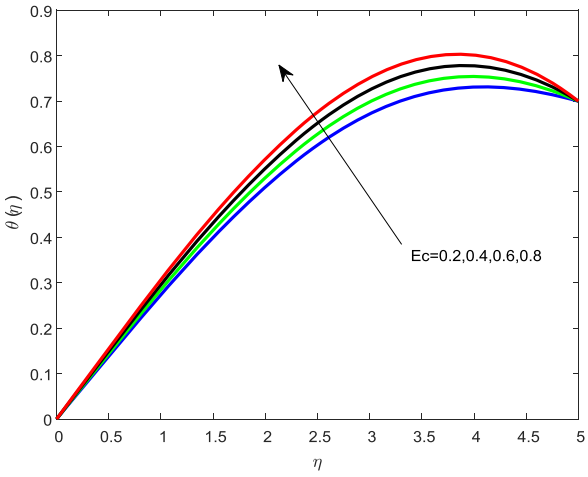

Figure 4. impact of Ec on $\theta(\eta)$

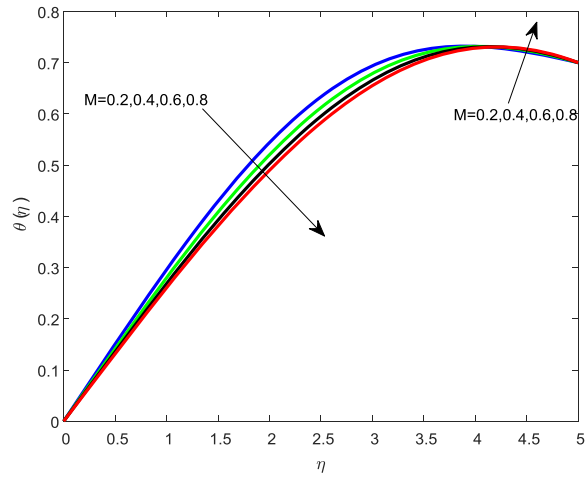

Figure 3. impact of M on $\theta(\eta)$

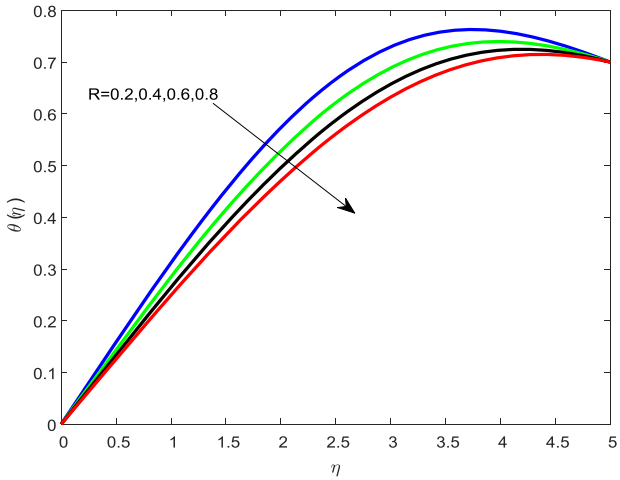

Figure 5. impact of R on $\theta(\eta)$

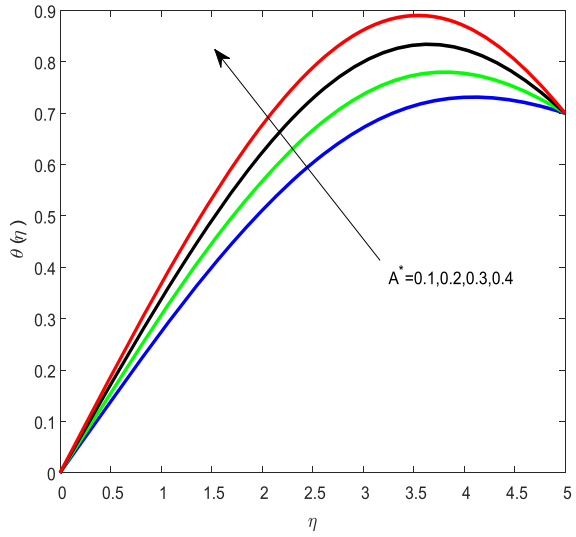

Figure 6. impact of A^* on $\theta(\eta)$

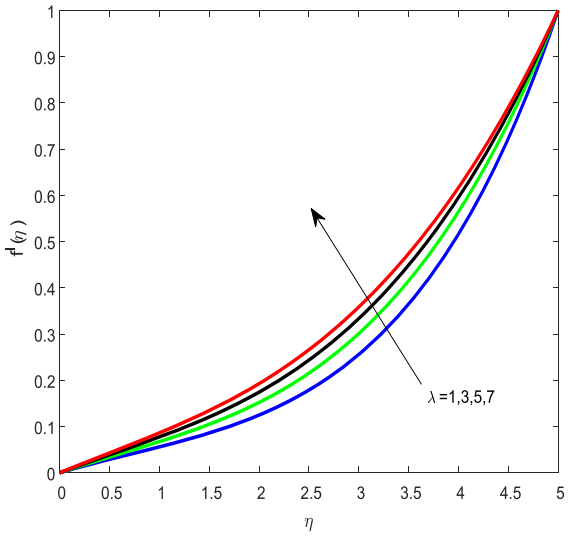

Figure 8. impact of λ on $f'(\eta)$

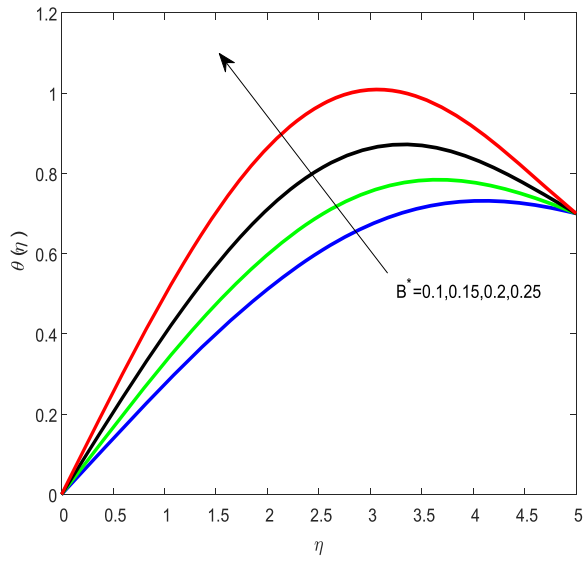

Figure 7. impact of B^* on $\theta(\eta)$

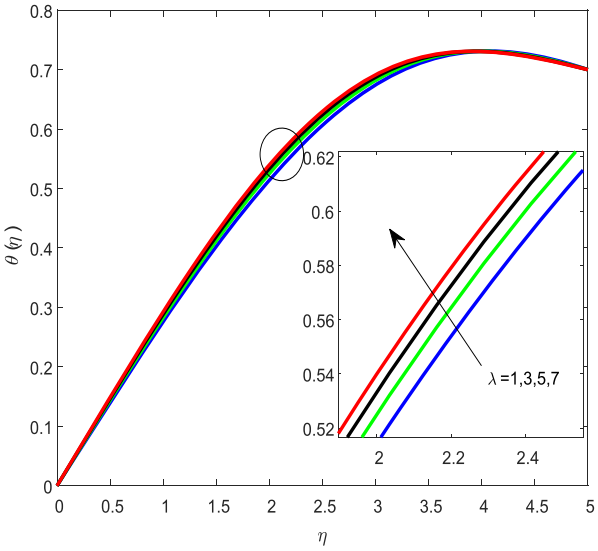

Figure 9. impact of λ on $\theta(\eta)$

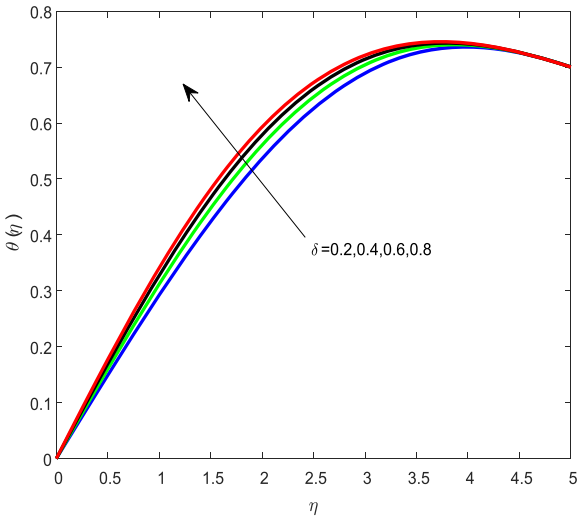

Figure 10. impact of δ on $\theta(\eta)$

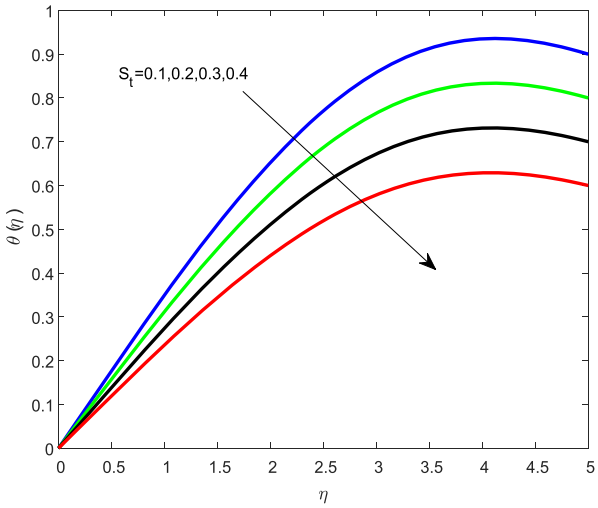

Figure 11. impact of Sr on $\theta(\eta)$

Table 1. Variations in $C_{f_x}R_{e_x}$ and $-\theta'(0)$ for Williamson fluid.

M	Ec	R	A^*	B^*	λ	δ	St	$C_{f_x}R_{e_x}$	$-\theta'(0)$
0.2								0.103117	-0.302238
0.4								0.071773	-0.284770
0.6								0.052900	-0.272642
	0.2							0.061162	-0.278149
	0.4							0.060370	-0.289559
	0.6							0.059579	-0.300902
		0.2						0.058796	-0.317799
		0.4						0.060492	-0.289276
		0.6						0.061746	-0.268543
			0.1					0.061162	-0.278149
			0.2					0.058978	-0.311712
			0.3					0.056877	-0.343786
				0.1				0.061162	-0.278149
				0.15				0.057807	-0.334899
				0.20				0.053445	-0.409479
					1			0.063723	-0.280341
					3			0.073066	-0.287693
					7			0.081474	-0.293606
						0.2		0.123293	-0.299492
						0.4		0.186801	-0.323361
						0.6		0.235803	-0.344328
							0.1	0.067438	-0.354497
							0.2	0.064313	-0.316408
							0.3	0.061162	-0.278149

4.Conclusions

- Rising values of M decreases the flow profile and mixing behavior in the thermal.
- Boosting values of R enhances the skin friction and reduced Nusselt number.
- An improved the Ec depreciates the flow and heat transfer**.**
- The activities of melting parameter on thermal profile is alike.
- $A^*$and B^* regulates the temperature boundary layer.

References

[1] Khan N A, Khan S and Riaz F (2014) *Math Sci Lett* **3** 199-205
[2] Krishnamurthy M R, Prasannakumara B C, Gireesha B J and Gorla R S R (2016) *Engg. Sci. and Tech. an Inter. J*. **16** 53-61
[3] Prasannakumara B C, Gireesha B J, Gorla R S R and Krishnamurthy M R (2016) *J. Aerosp. Eng,* DOI: 10.1061/(ASCE)AS. 1943-5525.0000578
[4] Bhatti M M and Rashidi M M (2016) *Jour. Mole. Liq.* **221** 567-573
[5] Nadeem S and Hussain S T (2014) *Appl Nanosci* **4** 1005-1012
[6] Hayat T, Shafiq A and Alsaedi A (2016) *Alex. Engg. J*. **55** 2229-2240
[7] Rashidi M M, Ganesh N V, Hakeem A K A and Ganga B (2014) *Journal of Molecular liquids* **198** 234-238.
[8] Zeeshan A, Majeed A and Ellahi R (2016) *Journal of Molecular liquids* **215** 549-554
[9] Sheikholeslami M, Ganji D D, Younus Javed M and Ellahi R (2015) *Journal of magnetism and Magnetic materials* **374** 36-43
[10] Pal D, Roy N and Vajravelu K (2016) *I. J. of Mech. Sci.* **114** 257-267
[11] Rashidi M M, Rostami B, Freidoonimehr N and Abbasbandy S (2014) *Ain Shams Engineering J*. **5** 901-912
[12] Hayat T, Waqas M, khan M I and Alsaedi A (2017) *J. Molecular Liquids* **225** 302-310
[13] Chamkha A, Mujtaba M, Quadri A and Issa C (2003) *Heat and Mass Transfer* **39** 305-312
[14] Cookey C. I, Ogulu A, and Omubo-Pepple V B (2003) *International Journal of Heat and Mass Transfer* **46(13)** 2305-2311
[15] Siddheshwar P G and Mahabaleswar U S (2005) *I. J. Non-Linear Mechanics* **40** 807-820
[16] Mabood F, Ibrahim S M, Rashidi M M, Shadloo M S and Lorenzini G (2016) *I. J.of. Heat and Mass Transfer* **93** 674-682
[17] Raju C S K, Sandeep N, Sulochana C,Sugunamma V and Jayachandra Babu (2015) *J. of the Nigerian Mathematical Society* **34** 169-180
[18] Mohan Krishna P, Sugunamma V and Sandeep N (2013) *Adv. Phy. Theori. and App*. **26**
[19] Reddy J V R, Sugunamma V, Sandeep N and Sulochana C (2016) *J. of the Nigerian Mathematical Society* **35** 48-65
[20] Raju R S, Ready G J, Rao J A and Rashidi M M (2016) *J. Comp. Desi. And Engg.* **3** 349-362
[21] Anjali Devi S P, Prakesh M (2015) *J. Niger. Math. Soc.*
[22] Animasaun I L, Sandeep N (2016) *Powder Technology* **301** 858-867
[23] Animasaun I L (2015) *Ain Shams Engineering Journal* **7(2),** 755–765
[24] Omowaye A J and Animasaun I L (2016) *Journal of Applied Fluid Mechanics* **9(4)** 1777–1790